A uniformly convergent scheme to solve two-dimensional parabolic singularly perturbed systems of reaction-diffusion type with multiple diffusion parameters

C. Clavero[1] and J.C. Jorge[2]

1 Department of Applied Mathematics and IUMA, University of Zaragoza, Zaragoza, Spain, email: clavero@unizar.es
2 Department of Computer Science, Mathematics and Statistics and ISC, Public University of Navarra, Pamplona, Spain, email: jcjorge@unavarra.es

Abstract

In this work we deal with solving two dimensional parabolic singularly perturbed systems of reaction–diffusion type where the diffusion parameters at each equation of the system can be small and of different scale. In such case, in general, overlapping boundary layers appear at the boundary of the spatial domain and, because of this, special meshes are required to resolve them. The numerical scheme combines the central difference scheme to discretize in space and the fractional implicit Euler method together with a splitting by components to discretize in time. If the fully discrete scheme is defined on an adequate piecewise uniform Shishkin mesh in space then it is uniformly convergent of first order in time and of almost second order in space. Some numerical results illustrate the theoretical results.

kEYWORDS fractional Euler method, reaction-diffusion parabolic systems, Shishkin meshes, splitting by components, uniform convergence.
AMS codes: 65N12, 65M06, 65N06

1 Introduction

We are interested in solving efficiently a class of 2D parabolic reaction-diffusion singularly perturbed coupled systems, with time dependent Dirichlet boundary conditions, which is defined as follows: Find $\mathbf{u} : \overline{\Omega} \times [0,T] \to \mathcal{R}^2$ solution of

$$\left\{ \begin{array}{l} L_\varepsilon \mathbf{u} \equiv \dfrac{\partial \mathbf{u}}{\partial t}(\mathbf{x},t) + \mathcal{L}_{\mathbf{x},\varepsilon}(t)\mathbf{u}(\mathbf{x},t) = \mathbf{f}(\mathbf{x},t),\ (\mathbf{x},t) \in Q \equiv \Omega \times (0,T], \\ \mathbf{u}(\mathbf{x},t) = \mathbf{g}(\mathbf{x},t),\ \mathbf{x} \in \partial\Omega,\ t \in (0,T],\ \mathbf{u}(\mathbf{x},0) = \boldsymbol{\varphi}(\mathbf{x}),\ \mathbf{x} \in \overline{\Omega}, \end{array} \right. \tag{1}$$

where $\mathbf{u} \equiv \mathbf{u}(\mathbf{x},t) = (u_1(\mathbf{x},t), u_2(\mathbf{x},t))^T$, $\mathbf{x} = (x,y)$, $\Omega = (0,1)^2$ and the spatial differential operator $\mathcal{L}_{\mathbf{x},\varepsilon}(t)$ is defined as

$$\mathcal{L}_{\mathbf{x},\varepsilon}(t)\mathbf{u} \equiv -\mathcal{D}\Delta\mathbf{u} + \mathcal{A}\mathbf{u},$$

with $\mathcal{D} = \text{diag}(\varepsilon_1, \varepsilon_2)$ and $\mathcal{A} \equiv \mathcal{A}(\mathbf{x}, t) = (a_{kr}(\mathbf{x}, t)) \in \mathcal{R}^{2\times 2}, k, r = 1, 2$.

We denote by $\boldsymbol{\varepsilon} = (\varepsilon_1, \varepsilon_2)^T$ the diffusion parameter vector, with $0 < \varepsilon_1 \leq \varepsilon_2 \leq 1$, and we assume that these parameters can be very small and even they can have different orders of magnitude. As well, we assume that the reaction matrix $\mathcal{A}$ is an M-matrix, i.e., for $(\mathbf{x}, t) \in \overline{Q}$ it holds

$$\sum_{r=1}^{2} a_{kr} \geq \alpha > 0,\ a_{kk} > 0,\ k = 1, 2,\ a_{kr} \leq 0, \quad \text{if} \quad k \neq r, \tag{2}$$

which is a usual hypothesis for coupled reaction-diffusion systems (see References [7, 10] for instance). Then, in general, overlapping boundary layers of widths $\mathcal{O}(\sqrt{\varepsilon_1})$ and $\mathcal{O}(\sqrt{\varepsilon_2})$ appear at the boundary $\partial\Omega$. Moreover, we suppose that the data $\mathbf{f}(\mathbf{x}, t) = (f_1, f_2)^T$, $\boldsymbol{\varphi}(\mathbf{x}) = (\varphi_1, \varphi_2)^T$, $\mathbf{g}(\mathbf{x}, t) = (g_1, g_2)^T$ and the reaction matrix $\mathcal{A}$ are sufficiently smooth functions, and also that sufficient compatibility conditions between them hold in order to $\mathbf{u} \in C^{4,2}(\overline{Q})$ (see Reference [12] for a detailed discussion).

Coupled singularly perturbed systems appear in mathematical models of many physical problems as saturated flow in fractured porous media, reaction-diffusion enzyme model or tubular model in chemical reactor theory (see Reference [13] for instance). In the literature, there are many works which analyze the use of efficient numerical methods to solve this type of problems; for 1D elliptic or parabolic problems see References [2, 7, 8, 11] and for 2D elliptic or parabolic problems see References [1, 3, 9, 10, 15]. Here, we construct an efficient numerical scheme, which reduces the computational cost of classical implicit methods by decoupling the components of the exact solution and also which eludes the order reduction which usually appears when some classical time integrators are used, specially in the presence of time dependent boundary conditions.

The article is structured as follows. In section 2, we describe the asymptotic behavior of the exact solution of the continuous problem, giving appropriate estimates for its derivatives with respect to the diffusion parameters. In Section 3, we discretize in space by using the classical central difference scheme defined on a nonuniform mesh of Shishkin type, proving that it is uniformly convergent of almost second order. In section 4, we discretize in time by using the fractional implicit Euler method and a splitting by components, see References [2, 3], and we prove that it is uniformly convergent of first order. In Section 5, numerical results for some test problems are shown, which corroborate in practice the theoretical results. Finally, in Section 6 some concluding remarks are given.

Henceforth, C denotes a positive constant independent of the diffusion parameters $\varepsilon_k,\ k = 1, 2$ and the discretization parameters N and M, and $\mathbf{C} = (C, C)^T$. Moreover, $\mathbf{v} \leq \mathbf{w}$ means that $v_k \leq w_k$, $k = 1, 2$, $|\mathbf{v}| = (|v_1|, |v_2|)^T$ and $\|\mathbf{f}\|_G = \max\{\|f_1\|_G, \|f_2\|_G\}$ where $\|f\|_G$ is the maximum norm of f on the closed set G; we will use $\mathbf{v} \leq \mathbf{C}$ meaning that $v_k \leq C,\ k = 1, 2$.

2 Asymptotic behavior of the exact solution

In this section, we detail the asymptotic behavior of the solution $\mathbf{u}$ of (1) and its derivatives; from them, we deduce that its solution has overlapping boundary layers of width $\mathcal{O}(\sqrt{\varepsilon_1})$ and $\mathcal{O}(\sqrt{\varepsilon_2})$ on the boundary $\partial\Omega$.

Such results derive from the following maximum principle for problem (1); the proof of this result follows the ideas in [7, 11] for the case of parabolic one dimensional problems.

Lemma 1. *(Maximum principle) Let $w \in C(\overline{Q}) \cap C^2(Q)$ be such that $\mathcal{L}_\varepsilon \mathbf{w} \geq \mathbf{0}$ on Q and $\mathbf{w} \geq \mathbf{0}$ on $\partial\Omega \times [0,T]$. Then, $\mathbf{w} \geq \mathbf{0}$, $\forall (x,t) \in \overline{Q}$.*

To give precise estimates for spatial derivatives, we make use of the following boundary layer function

$$B_\mu(z) = e^{-\sqrt{\alpha}z/\sqrt{\mu}} + e^{-\sqrt{\alpha}(1-z)/\sqrt{\mu}} \tag{3}$$

Then, a detailed analysis (see Reference [4] for a full proof), which uses similar ideas to [3, 7, 10], proves estimates for the derivatives of the exact solution, which are needed in the subsequent analysis of the uniform convergence of our numerical algorithm .

Theorem 1. *The components of the exact solution $\mathbf{u}$ of (1) satisfy*

$$\left| \frac{\partial^l u_k}{\partial t^l} \right| \leq C, \ k = 1,2, \ 0 \leq l \leq 2, \tag{4}$$

and

$$\begin{aligned}
&\left| \frac{\partial^l u_1}{\partial x^l} \right| \leq C \left(1 + \varepsilon_1^{-l/2} B_{\varepsilon_1}(x) + \varepsilon_2^{-l/2} B_{\varepsilon_2}(x) \right), \ l = 1,2,3,4, \\
&\left| \frac{\partial^l u_2}{\partial x^l} \right| \leq C \left(1 + \varepsilon_2^{-l/2} B_{\varepsilon_2}(x) \right), \ l = 1,2, \\
&\left| \frac{\partial^l u_2}{\partial x^l} \right| \leq C \left(1 + \varepsilon_2^{-1} \left(\varepsilon_1^{1-l/2} B_{\varepsilon_1}(x) + \varepsilon_2^{1-l/2} B_{\varepsilon_2}(x) \right) \right), \ l = 3,4, \\
&\left| \frac{\partial^l u_1}{\partial y^l} \right| \leq C \left(1 + \varepsilon_1^{-l/2} B_{\varepsilon_1}(y) + \varepsilon_2^{-l/2} B_{\varepsilon_2}(y) \right), \ l = 1,2,3,4, \\
&\left| \frac{\partial^l u_2}{\partial y^l} \right| \leq C \left(1 + \varepsilon_2^{-l/2} B_{\varepsilon_2}(y) \right), \ l = 1,2, \\
&\left| \frac{\partial^l u_2}{\partial y^l} \right| \leq C \left(1 + \varepsilon_2^{-1} \left(\varepsilon_1^{1-l/2} B_{\varepsilon_1}(y) + \varepsilon_2^{1-l/2} B_{\varepsilon_2}(y) \right) \right), \ l = 3,4,
\end{aligned} \tag{5}$$

where C is a positive constant independent of the diffusion parameters ε_k, $k = 1,2$.

3 The spatial discretization on a Shishkin mesh

To discretize in space problem (1), we use the classical central difference scheme. As the exact solution, in general, has overlapping parabolic boundary layers on $\partial\Omega$, we use a piecewise uniform mesh of Shishkin type, $\overline{\Omega}^N \equiv I_{x,\varepsilon,N} \times I_{y,\varepsilon,N}$, which concentrates appropriately the grid points in the boundary layer regions. Such grids are defined as tensor products of one dimensional piecewise uniform Shishkin meshes, $I_{x,\varepsilon,N} = \{0 = x_0 < \ldots < x_N = 1\}$, $I_{y,\varepsilon,N} = \{0 = y_0 < \ldots < y_N = 1\}$, being N the discretization parameter which is a positive integer multiple of 8. For simplicity, we assume that the number of grid points in both spatial directions is the same.

The mesh $I_{x,\varepsilon,N}$ (analogously $I_{y,\varepsilon,N}$) uses the transition parameters

$$\sigma_{\varepsilon_2} = \min\{1/2, \sigma_0\sqrt{\varepsilon_2}\ln N\}, \quad \sigma_{\varepsilon_1} = \min\{\sigma_{\varepsilon_2}/2, \sigma_0\sqrt{\varepsilon_1}\ln N\}. \tag{6}$$

with σ_0 a constant to be fixed later. Then, the grid points are given by

$$x_i = \begin{cases} ih_{\varepsilon_1}, & i = 0, \ldots, N/8, \\ x_{N/8} + (i - N/8)h_{\varepsilon_2}, & i = N/8+1, \ldots, N/4, \\ x_{N/4} + (i - N/4)H, & i = N/4+1, \ldots, 3N/4, \\ x_{3N/4} + (i - 3N/4)h_{\varepsilon_2}, & i = 3N/4+1, \ldots, 7N/8, \\ x_{7N/8} + (i - 7N/8)h_{\varepsilon_1}, & i = 7N/8+1, \ldots, N, \end{cases} \tag{7}$$

where $H = 2(1 - \sigma_{\varepsilon_2})/N$, $h_{\varepsilon_2} = 8(\sigma_{\varepsilon_2} - \sigma_{\varepsilon_1})/N$, $h_{\varepsilon_1} = 8\sigma_{\varepsilon_1}/N$. We denote by $h_{x,i} = x_i - x_{i-1}$, $i = 1, \ldots, N$, and $\overline{h}_{x,i} = (h_{x,i} + h_{x,i+1})/2$, $i = 1, \ldots, N-1$.

Let us denote by Ω^N the subgrid of $\overline{\Omega}^N$ composed only by the interior points of it, i.e., by $\overline{\Omega}^N \bigcap \Omega$, $\partial\Omega^N = \overline{\Omega}^N \bigcap \partial\Omega$, by $[\mathbf{v}]_{\Omega^N}$ the restriction operators, applied to vector functions defined on Ω, to the mesh Ω^N, and by $[\mathbf{v}]_{\partial\Omega^N}$ the restriction operators, applied to vector functions defined on $\partial\Omega$, to the mesh $\partial\Omega^N$. On the mesh Ω^N, we introduce the semidiscretization approach $\mathbf{U}^N(t) \equiv \left(\mathbf{U}^N_{i,j}(t)\right)_{i,j=1,\ldots N-1}$, being $\mathbf{U}^N_{i,j}(t) \equiv (U_{i,j,1}.U_{i,j,2})^T$ the approximations of $\mathbf{u}(x_i, y_j, t)$, which compose the solution of the initial value problem

$$\begin{cases} \dfrac{d\mathbf{U}^N}{dt}(t) + \mathcal{L}^N_\varepsilon(t)\overline{\mathbf{U}}^N(t) = [\mathbf{f}(\mathbf{x}, t)]_{\Omega^N}, \ \text{ in } \ \Omega^N \times [0, T], \\ \overline{\mathbf{U}}^N(t) = [\mathbf{g}(\mathbf{x}, t)]_{\partial\Omega^N}, \ \text{ in } \ \partial\Omega^N \times [0, T], \\ \mathbf{U}^N(0) = [\varphi(\mathbf{x})]_{\Omega^N}, \end{cases} \tag{8}$$

where $\overline{\mathbf{U}}^N(t)$ represents the natural extension to $\overline{\Omega}^N \times [0, T]$ of the semidiscrete functions $\mathbf{U}^N(t)$, defined on $\Omega^N \times [0, T]$, by adding the corresponding boundary data. As well, $\mathcal{L}^N_\varepsilon(t)$ is the discretization of the operator $\mathcal{L}_{x,\varepsilon}(t)$ using the central differences scheme, that is,

$$\begin{aligned} (\mathcal{L}^N_\varepsilon(t)\overline{\mathbf{U}}^N)_{i,j,k} = c_{i,j,l,k}U^N_{i-1,j,k} + c_{i,j,r,k}U^N_{i+1,j,k} + c_{i,j,d,k}U^N_{i,j-1,k} + \\ c_{i,j,u,k}U^N_{i,j+1,k} + c_{i,j,c,k}U^N_{i,j,k} + a_{k1}(t)U^N_{i,j,1} + a_{k2}(t)U^N_{i,j,2}, \ k = 1, 2, \end{aligned} \tag{9}$$

with

$$c_{i,j,l,k} = \frac{-\varepsilon_k}{h_{x,i}\overline{h}_{x,i}}, c_{i,j,r,k} = \frac{-\varepsilon_k}{h_{x,i+1}\overline{h}_{x,i}}, c_{i,j,d,k} = \frac{-\varepsilon_k}{h_{y,j}\overline{h}_{y,j}}, c_{i,j,u,k} = \frac{-\varepsilon_k}{h_{y,j+1}\overline{h}_{y,j}},$$
$$c_{i,j,c,k} = -(c_{i,j,l,k} + c_{i,j,r,k} + c_{i,j,d,k} + c_{i,j,u,k}),\ k = 1, 2, \tag{10}$$

where $a_{kr}(t) = a_{kr}(x_i, y_j, t),\ k, r = 1, 2$ and $i, j = 1, \ldots N-1$.

The uniform well-posedness of (8) is a consequence of the following semidiscrete maximum principle (see Reference [3]).

Theorem 2. *Under the assumption* $[\mathbf{f}(\mathbf{x}, t)]_{\Omega^N} \leq \mathbf{0}$*, it holds that* $\overline{\mathbf{U}}^N(t)$ *reaches its maximum componentwise value at the boundary* $\partial\Omega^N \times [0, T] \bigcup \Omega^N \times \{0\}$.

Theorem 3. *If* $[\mathbf{f}(\mathbf{x}, t)]_{\Omega^N} \geq \mathbf{0}$*,* $[\mathbf{g}(\mathbf{x}, t)]_{\partial\Omega^N} \geq \mathbf{0}$ *and* $[\boldsymbol{\varphi}(\mathbf{x})]_{\Omega^N} \geq \mathbf{0}$*, then* $\overline{\mathbf{U}}^N(t) \geq \mathbf{0}$.

Using a well known barrier-function technique, see Reference [14] for instance, the following result can be obtained.

Theorem 4. *(Uniform stability). The unique solution of problem (8) satisfies the uniform bound*

$$\|\overline{\mathbf{U}}^N(t)\|_{\overline{\Omega}^N \times [0,T]} \leq$$
$$\max\{\|[\boldsymbol{\varphi}(x)]_{\Omega^N}\|_{\Omega^N}, \|[\mathbf{g}(x,t)]_{\partial\Omega^N}\|_{\partial\Omega^N \times [0,T]}, \frac{1}{\alpha}\|[\mathbf{f}(x,t)]_{\Omega^N}\|_{\Omega^N \times [0,T]}\}.$$

Using the previous results and a fine analysis of the local truncation error associated to the central difference scheme, we conjecture that the global error associated to the spatial discretization defined on the previous Shishkin mesh satisfies

$$\|[\mathbf{u}(x,t)]_{\Omega^N} - \mathbf{U}^N(t)\|_{\Omega_N} \leq CN^{-2}\ln^2 N, \quad \forall\ t \in [0, T], \tag{11}$$

where C is independent of $\boldsymbol{\varepsilon}$ and N (in Reference [4] we will include a detailed proof of this result).

4 The fully discrete scheme: uniform convergence

In this section, we describe in detail the numerical algorithm which we propose to solve (1). To simplify the expressions, we introduce the difference operators

$$\mathcal{L}^N_{x,1}(t)v^N \equiv -\varepsilon\partial_{xx}v^N + a_{x,11}(t)v^N,\ \mathcal{L}^N_{y,1}(t)v^N \equiv -\varepsilon\partial_{yy}v^N + a_{y,11}(t)v^N,$$
$$\mathcal{L}^N_{x,2}(t)v^N \equiv -\varepsilon\partial_{xx}v^N + a_{x,22}(t)v^N,\ \mathcal{L}^N_{y,2}(t)v^N \equiv -\varepsilon\partial_{yy}v^N + a_{y,22}(t)v^N,$$

being ∂_{xx} and ∂_{yy} the classical second order central differences on the corresponding one dimensional Shishkin meshes, with $a_{x,kk}(x, y, t) + a_{y,kk}(x, y, t) = a_{kk}(x, y, t), k =$

$1,2$. We will choose that $a_{z,kk}(x,y,t) \geq 0,\ k=1,2, z=x,y$. Analogously, we decompose the non diagonal coefficients of the reaction matrix in the form $a_{x,kr}(x,y,t)+a_{y,kr}(x,y,t)=a_{kr}(x,y,t),\ k,r=1,2, k\neq r$, choosing that $a_{z,kr}(x,y,t)\leq 0,\ k,r=1,2, k\neq r, z=x,y$, and $\sum_{r=1}^{2} a_{z,kr}(x,y,t)\geq \alpha_z > 0, k=1,2, z=x,y$ ($\alpha_x+\alpha_y=\alpha$). As well, we decompose the right-hand side $\mathbf{f}(\mathbf{x},t)\equiv (f_1,f_2)^T$, in the form $\mathbf{f}_x(\mathbf{x},t)+\mathbf{f}_y(\mathbf{x},t)\equiv (f_{x,1},f_{x,2})^T+(f_{y,1},f_{y,2})^T$.

Then, by using the fractional implicit Euler method and a splitting by components, the fully discrete scheme is given by

$$
\begin{array}{l}
\text{(initialize)}\ \ \mathbf{U}^{N,0}=[\boldsymbol{\varphi}]_{\Omega^N},\\
\left\{\begin{array}{l}
\text{(first half step)}\\
(I+\tau\mathcal{L}^N_{x,1}(t_{m+1}))\overline{U}^{N,m+1/2}_1 = U^{N,m}_1+\tau F^{m+1}_{x,1}-\tau a_{x,12}(t_{m+1})U^{N,m}_2,\ \ \text{in } \Omega^N,\\
(I+\tau\mathcal{L}^N_{x,2}(t_{m+1}))\overline{U}^{N,m+1/2}_2 = U^{N,m}_2+\tau F^{m+1}_{x,2}-\tau a_{x,21}(t_{m+1})U^{N,m+1/2}_1, \text{in } \Omega^N,\\
\overline{\mathbf{U}}^{N,m+1/2}_{0,j}=\mathbf{G}^{N,m+1/2}_{0,j}, \overline{\mathbf{U}}^{N,m+1/2}_{N,j}=\mathbf{G}^{N,m+1/2}_{N,j}, j=1,\ldots,N-1,\\
\text{(second half step)}\\
(I+\tau\mathcal{L}^N_{y,2}(t_{m+1}))\overline{U}^{N,m+1}_2 = U^{N,m+1/2}_2+\tau F^{m+1}_{y,2}-\tau a_{y,21}(t_{m+1})U^{N,m+1/2}_1, \text{in } \Omega^N,\\
(I+\tau\mathcal{L}^N_{y,1}(t_{m+1}))\overline{U}^{N,m+1}_1 = U^{N,m+1/2}_1+\tau F^{m+1}_{y,1}-\tau a_{y,12}(t_{m+1})U^{N,m+1}_2, \text{in } \Omega^N,\\
\overline{\mathbf{U}}^{N,m+1}_{i,j}=\mathbf{g}(x_i,y_j,t_{m+1}), \qquad (x_i.y_j)\in\partial\Omega^N,\\
\qquad\qquad\qquad\qquad\qquad\qquad m=0,\ldots,M-1,
\end{array}\right.
\end{array}
\tag{12}
$$

where $\tau\equiv T/M$ is the time step, $t_m=m\tau$, are the intermediate times and the semidiscrete solutions $\overline{\mathbf{U}}(t_{m+1})$ are going to be approached by $\overline{\mathbf{U}}^{N,m+1}, m=0,\ldots,M-1$. The contributions of the source term to right-hand sides are

$$
F^{m+1}_{z,k}\equiv [f_{z,k}(\mathbf{x},t_{m+1})]_{\Omega^N}, k=1,2, z=x,y,
\tag{13}
$$

and the discrete boundary data for the first half step are given by

$$
\begin{array}{rl}
\mathbf{G}^{N,m+1/2}_0 = \big(&((I+\tau\mathcal{L}^N_{y,1}(t_{m+1}))[g_1(0,y,t_{m+1})]_{\bar{I}_y}-\tau[f_{y,1}(0,y,t_{m+1})]_{I_y}+\\
&[\tau a_{y,12}(0,y,t_{m+1})g_2(0,y,t_{m+1})]_{I_y},\\
&\qquad (I+\tau\mathcal{L}^N_{y,2}(t_{m+1}))[g_2(0,y,t_{m+1})]_{\bar{I}_y}-\tau[f_{y,2}(0,y,t_{m+1})]_{I_y}+\\
&[\tau a_{y,21}(0,y,t_{m+1})g_1(0,y,t_{m+1})]_{I_y}\big)^T,
\end{array}
\tag{14}
$$

$$
\begin{array}{rl}
\mathbf{G}^{N,m+1/2}_N = \big(&((I+\tau\mathcal{L}^N_{y,1}(t_{m+1}))[g_1(1,y,t_{m+1})]_{\bar{I}_y}-\tau[f_{y,1}(1,y,t_{m+1})]_{I_y}+\\
&[\tau a_{y,12}(1,y,t_{m+1})g_2(1,y,t_{m+1})]_{I_y},\\
&\qquad (I+\tau\mathcal{L}^N_{y,2}(t_{m+1}))[g_2(1,y,t_{m+1})]_{\bar{I}_y}-\tau[f_{y,2}(1,y,t_{m+1})]_{I_y}+\\
&[\tau a_{y,21}(1,y,t_{m+1})g_1(1,y,t_{m+1})]_{I_y}\big)^T.
\end{array}
\tag{15}
$$

This special choice of the boundary data is motivated by the order reduction effect which appears when standard evaluations of the boundary data are chosen (see Reference [3]).

Notice that only tridiagonal linear systems are involved in (12) to obtain the numerical solution $\mathbf{U}^{N,\bullet}$ at each time level of the discretization. This fact provokes that the computational cost of our method is significantly smaller in comparison with the cost of classical implicit methods, for which large block tridiagonal systems must be solved.

In Reference [4] we will give full details for proving that, under the assumptions made on the splitting of the reaction terms $a_{z,kr}, z = x, y, k, r = 1, 2$, the time integration process (12) is contractive and uniformly consistent of order one. Combining these two properties in a well-known way, it can be deduced that the time integration process (12) is a first order uniformly convergent method, that is, it holds

$$\|\overline{\mathbf{U}}^{N}(t_m) - \overline{\mathbf{U}}^{N,m}\|_{\overline{\Omega}^N} \leq CM^{-1}, \tag{16}$$

being C a constant independent of ε, N and M.

Combining (11) and (16), we deduce that the global error associated to the fully discrete scheme defined by (12-15) on the Shishkin mesh satisfies

$$\max_{0\leq m\leq M} \|\overline{\mathbf{U}}^{N,m} - [\mathbf{u}(x,t_m)]_{\overline{\Omega}^N}\|_{\overline{\Omega}^N} \leq C\left(N^{-2}\ln^2 N + M^{-1}\right), \tag{17}$$

where the constant C is independent of the diffusion parameter $\boldsymbol{\varepsilon}$ and the discretization parameters N and M. Then, the fully discrete scheme is a uniformly convergent method, which has first order in time and almost second order in space.

5 Numerical results

In this section, we show the numerical results obtained with our algorithm for some test problems of type (1). The data for the first example are

$$\begin{aligned}
&\mathcal{A}(\mathbf{x},t) = \begin{pmatrix} 4+x^2y^2t & -x^2y^2t \\ -2x^2y^2t^2 & 3+x^2y^2t^2 \end{pmatrix},\ \mathbf{x}\in\Omega,\ t\in(0,1],\\
&\mathbf{f}(\mathbf{x},t) = \begin{pmatrix} x^2y^2(1-x)(1-y)t^2 \\ xy(1-x)(1-y)(1-e^{-t})^2) \end{pmatrix},\ \mathbf{x}\in\Omega,\ t\in(0,1],\\
&\mathbf{g}(\mathbf{x},t) = \begin{pmatrix} (x^2y^2+1)(1+t) \\ (x+y+1)(2-t^2)^2) \end{pmatrix},\ \mathbf{x}\in\partial\Omega,\ t\in(0,1],\\
&\boldsymbol{\varphi}(\mathbf{x}) = \begin{pmatrix} x^2y^2+1 \\ 4(x+y+1) \end{pmatrix},\ \mathbf{x}\in\overline{\Omega}.
\end{aligned} \tag{18}$$

Figure 1 displays the numerical solution at the final time $t = 1$ for some values of the diffusion parameters. In it, the boundary layers at the boundary of the spatial domain can be observed.

Figure 1: Components U_1 (left) and U_2 (right) at $t = 1$ for example (18) with $\varepsilon_1 = 10^{-5}, \varepsilon_2 = 10^{-3}$ and $N = M = 32$

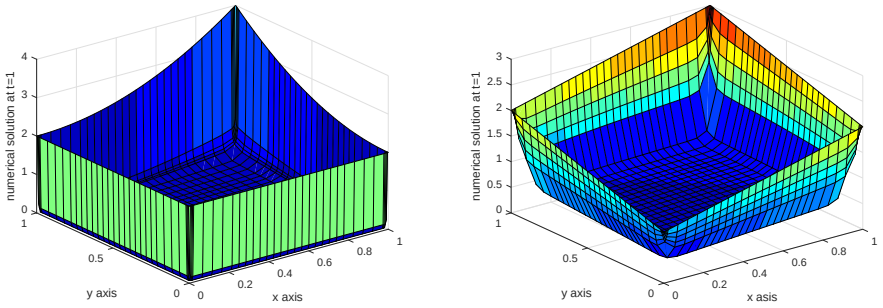

To observe more in detail the boundary layers of the solution, we show two additional pictures. Figure 2 displays the numerical solution at time $t = 1$ taking a fixed value of y corresponding to the grid point $y_{N/8}$ for the full interval and a zoom near $x = 0$; Figure 3 displays the numerical solution at time $t = 1$ taking a fixed value of x corresponding to the grid point $x_{3N/8}$ for the full interval and a zoom near $y = 1$. From both, we clearly see the boundary layers at the end points and also that the boundary layers of the first component are sharper than the ones of the second component.

Figure 2: Components U_1 and U_2 at $t = 1$ for example (18) with y fixed, $\varepsilon_1 = 10^{-5}, \varepsilon_2 = 10^{-3}$ and $N = M = 64$

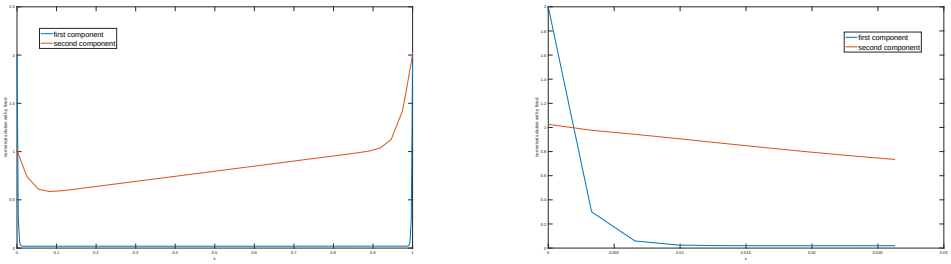

Figure 3: Components U_1 and U_2 at $t = 1$ for example (18) with x fixed, $\varepsilon_1 = 10^{-5}, \varepsilon_2 = 10^{-3}$ and $N = M = 64$

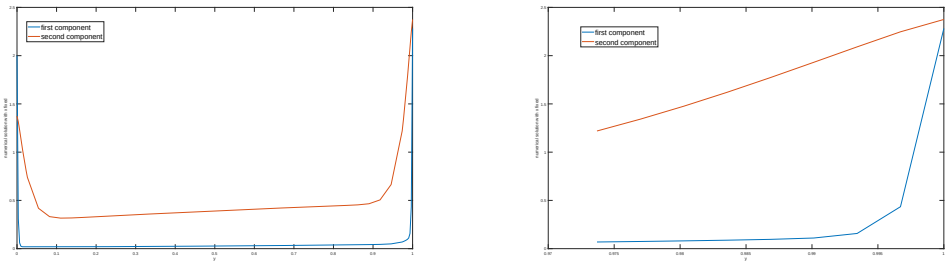

To see how the solutions evolve in time, figures 4, 5 and 6 display the solution at three different times, taking the same values of the discretization and the diffusion parameters as in Figure 1.

Figure 4: Components U_1 (left) and U_2 (right) at $t = 0.25$ for example (18) with $\varepsilon_1 = 10^{-5}, \varepsilon_2 = 10^{-3}$ and $N = M = 32$

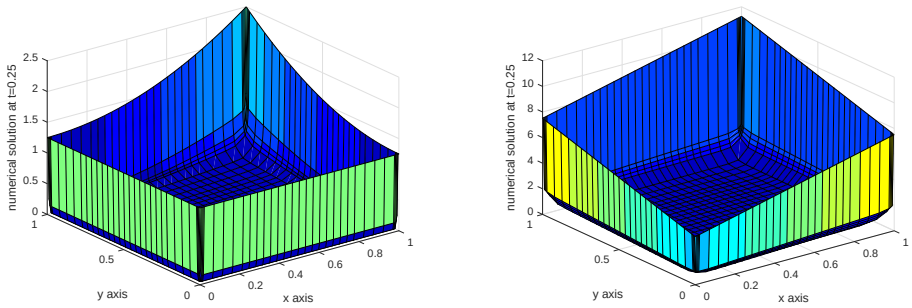

As well, Figure 7 displays the evolution in time of the components $U_1(\sigma_{\varepsilon_1}, \sigma_{\varepsilon_2}, t)$ and $U_2(\sigma_{\varepsilon_1}, \sigma_{\varepsilon_2}, t)$ for $0 \leq t \leq 1$, for the same values of the discretization and the diffusion parameters as in Figure 1.

In the construction of the algorithm, we need a suitable smooth partition of the reaction matrix; here, for simplicity, we have chosen

$$a_{x,kr}(x, y, t) = a_{y,kr}(x, y, t) = a_{kr}(x, y, t)/2, \;\; k, r = 1, 2. \tag{19}$$

Moreover, we also need a partition of $\mathbf{f}(\mathbf{x}, t) \equiv (f_1, f_2)^T$, in the form $\mathbf{f}_x + \mathbf{f}_y \equiv$

Figure 5: Components U_1 (left) and U_2 (right) at $t = 0.5$ for example (18) with $\varepsilon_1 = 10^{-5}, \varepsilon_2 = 10^{-3}$ and $N = M = 32$

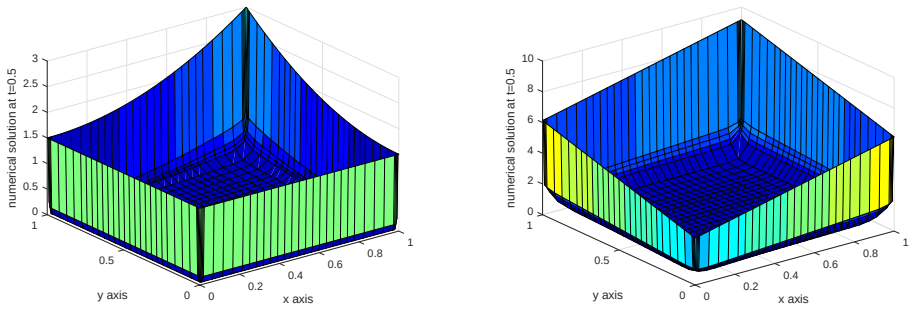

Figure 6: Components U_1 (left) and U_2 (right) at $t = 0.75$ for example (18) with $\varepsilon_1 = 10^{-5}, \varepsilon_2 = 10^{-3}$ and $N = M = 32$

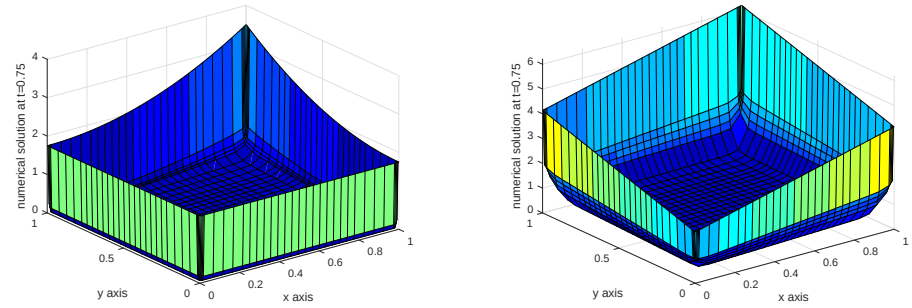

$(f_{x,1}, f_{x,2})^T + (f_{y,1}, f_{y,2})^T$. Here, following to Reference [5], we have used

$$\begin{aligned} f_{y,k}(x,y,t) &= f_k(x,0,t) + y(f_k(x,1,t) - f_k(x,0,t)), \\ f_{x,k}(x,y,t) &= f_k(x,y,t) - f_{k,y}(x,y,t),\ k = 1,2. \end{aligned} \tag{20}$$

Nevertheless, any other smooth partition would be also valid here.

As the exact solution of problem (1) is unknown, we cannot calculate the errors exactly; to approximate them, we use a variant of the double-mesh principle (see Reference [6]). The maximum errors and the maximum uniform errors are approximated by

$$d_{\boldsymbol{\varepsilon},k}^{N,M} = \max_{0\le m\le M} \max_{0\le i,j\le N} |U_{i,j,k}^{N,M} - \widehat{U}_{2i,2j,k}^{2N,2M}|,\ k = 1,2,\ \ d_k^{N,M} = \max_{\varepsilon} d_{\boldsymbol{\varepsilon},k}^{N,M},\ k = 1,2,$$

Figure 7: Components $U_1(\sigma_{\varepsilon_1}, \sigma_{\varepsilon_2}, t)$ (left) and $U_2(\sigma_{\varepsilon_1}, \sigma_{\varepsilon_2}, t)$ (right) for example (18) with $\varepsilon_1 = 10^{-5}, \varepsilon_2 = 10^{-3}$ and $N = M = 32$

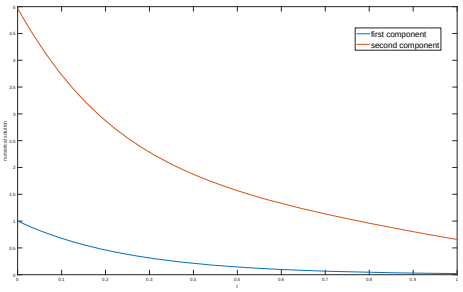

where $\{\widehat{\mathbf{U}}_{i,j}^{2N,2M}\}$ is the numerical solution on a finer mesh $\{(\hat{x}_i, \hat{y}_j, \hat{t}_m)\}$, which has the grid points of the coarse mesh and their midpoints. From the double-mesh differences we obtain the corresponding orders of convergence and the $\boldsymbol{\varepsilon}$-uniform orders of convergence

$$p_k = \log(d_{\boldsymbol{\varepsilon},k}^{N,M}/d_{\boldsymbol{\varepsilon},k}^{2N,2M})/\log 2,\ k = 1, 2,\ \ p_k^{uni} = \log(d_k^{N,M}/d_k^{2N,2M})/\log 2,\ k = 1, 2.$$

Table 1 shows the maximum errors and the orders of convergence for some values of ε_2, taking $\sigma_0 = 2$ in (6); for each value of ε_2, the diffusion parameter ε_1 is in the set $R = \{\varepsilon_1; \varepsilon_1 = \varepsilon_2, 10^{-1}\varepsilon_2, \ldots, 10^{-7}\}$. For each value of ε_2, the first and second rows correspond to the first component and the third and the fourth ones to the second one. From it, we see the almost first order of uniform convergence according to the theoretical results. This fact indicates that, from a numerical point of view, the errors associated to the time integration process dominate in the global errors.

To show the orders of convergence of the spatial discretization we must reduce the influence of the errors in time; Table 2 shows the results when the discretization parameter N is multiplied by 2, but the discretization parameter M is multiplied by 4. From it, we see that orders of uniform convergence are bigger than in Table 1, according to the theoretical results.

The theoretical analysis in this work only considers the case of systems with two equations. Nevertheless, this technique can be easily extended to systems with a larger number of equations. To illustrate numerically this fact, we consider a second example for a coupled system which has three equations. The data of this test

Table 1: Estimated maximum errors using the double mesh principle and orders of convergence for example (18)

ε_2	N=16 M=4	N=32 M=8	N=64 M=16	N=128 M=32	N=256 M=64
10^{-1}	2.2401E-1 0.1223 4.5168E-1 0.7504	2.0581E-1 0.4750 2.6850E-1 0.7699	1.4807E-1 0.6714 1.5746E-1 0.8096	9.2970E-2 1.1168 8.9838E-2 0.8638	4.2871E-2 4.9367E-2
10^{-2}	2.2798E-1 0.1431 6.0243E-1 0.6317	2.0645E-1 0.4687 3.8881E-1 0.9096	1.4918E-1 0.6635 2.0697E-1 0.9706	9.4186E-2 1.1011 1.0561E-1 0.9567	4.3907E-2 5.4414E-2
10^{-3}	2.3693E-1 0.2227 6.0821E-1 0.2654	2.0304E-1 0.4447 5.0601E-1 0.8109	1.4918E-1 0.6625 2.8844E-1 1.0294	9.4248E-2 1.0993 1.4131E-1 1.0990	4.3990E-2 6.5968E-2
10^{-4}	2.4520E-1 0.2795 6.2915E-1 0.2729	2.0202E-1 0.4396 5.2073E-1 0.7002	1.4896E-1 0.6619 3.2050E-1 1.2346	9.4146E-2 1.0987 1.3620E-1 1.0545	4.3959E-2 6.5574E-2
10^{-5}	2.4792E-1 0.2984 5.9729E-1 0.4519	2.0159E-1 0.4401 4.3668E-1 0.7854	1.4859E-1 0.6619 2.5335E-1 0.9495	9.3911E-2 1.0986 1.3119E-1 0.9983	4.3855E-2 6.5673E-2
$d_1^{N,M}$ p_1^{uni}	2.4792E-1 0.2641	2.0645E-1 0.4687	1.4918E-1 0.6626	9.4248E-2 1.0993	4.3990E-2
$d_2^{N,M}$ p_2^{uni}	6.2915E-1 0.2729	5.2073E-1 0.7002	3.2050E-1 1.1815	1.4131E-1 1.0990	6.5968E-2

problem are given by

$$
\begin{aligned}
\mathcal{A} &= \begin{pmatrix} e^{x+y}(1+t) & -(x+y)t & -tx \\ -(x+y) & (3+x+y)(1+t) & -t\sin(y) \\ -xy^2 & -t(\sin(x)+\sin(y)) & e^t(2+\cos(x+y)) \end{pmatrix}, \\
\mathbf{f}(\mathbf{x},t) &= \begin{pmatrix} 4t\cos(xy) \\ 5e^{-xyt}(1+x^2+y^2+t^2) \\ 4(\cos(xt)+\sin(yt)) \end{pmatrix}, \ \mathbf{x}\in\Omega, \ t\in(0,1], \\
\mathbf{g}(\mathbf{x},t) &= \begin{pmatrix} 4(x+y)\sin(t) \\ xyt^2 \\ 3e^{xy}(1-e^{-t}) \end{pmatrix}, \ \mathbf{x}\in\partial\Omega, \ t\in(0,1]. \\
\boldsymbol{\varphi}(\mathbf{x}) &= \mathbf{0}, \ \mathbf{x}\in\overline{\Omega}.
\end{aligned}
\tag{21}
$$

Again the exact solution of this problem is unknown. Figure 8 displays the numerical approximation for the three components, showing the boundary layers at the boundary of the spatial domain.

To obtain the numerical solutions, we have used the same ideas as in Reference [2] for coupled systems with more components. The fully discrete scheme uses again

Table 2: Estimated maximum errors using the double mesh principle and orders of convergence for example (18)

ε_2	N=16 M=4	N=32 M=16	N=64 M=64	N=128 M=256	N=256 M=1024
10^{-1}	2.2401E-1 0.3032 4.5168E-1 1.3762	1.8156E-1 0.5861 1.7401E-1 1.6443	1.2094E-1 0.7419 5.5663E-2 1.8317	7.2318E-2 1.2718 1.5638E-2 1.9215	2.9951E-2 4.1281E-3
10^{-2}	2.2798E-1 0.3284 6.0243E-1 0.9346	1.8157E-1 0.5827 3.1517E-1 1.6089	1.2124E-1 0.7422 1.0333E-1 1.8118	7.2478E-2 1.2717 2.9432E-2 1.9579	3.0019E-2 7.5759E-3
10^{-3}	2.3693E-1 0.4187 6.0821E-1 0.0284	1.7724E-1 0.5486 5.9637E-1 0.7100	1.2118E-1 0.7417 3.6458E-1 1.4525	7.2468E-2 1.2714 1.3321E-1 1.6333	3.0021E-2 4.2941E-2
10^{-4}	2.4520E-1 0.4756 6.2915E-1 0.0410	1.7634E-1 0.5428 6.1153E-1 0.6184	1.2105E-1 0.7409 3.9833E-1 1.1142	7.2431E-2 1.2711 1.8401E-1 1.5035	3.0012E-2 6.4900E-2
10^{-5}	2.4792E-1 0.4908 5.9729E-1 0.7986	1.7642E-1 0.5457 3.4339E-1 1.1249	1.2086E-1 0.7401 1.5745E-1 1.3923	7.2359E-2 1.2703 5.9984E-2 1.5561	2.9997E-2 2.0398E-2
$d_1^{N,M}$ p_1^{uni}	2.4792E-1 0.4493	1.8157E-1 0.5827	1.2124E-1 0.7422	7.2478E-2 1.2716	3.0021E-2
$d_2^{N,M}$ p_2^{uni}	6.2915E-1 0.0410	6.1153E-1 0.6184	3.9833E-1 1.1142	1.8401E-1 1.5035	6.4900E-2

a piecewise Shishkin adapted to the three overlapping boundary layers that form part of the exact solution of (1)-(21); for its definition, again a constant σ_0 must be chosen; in the following tables we have taken $\sigma_0 = 1$.

To approximate the maximum errors we use again the double mesh principle. Table 3 shows the maximum errors and the numerical orders of convergence for the first component, Table 4 for the second component and Table 5 for the third component, for some values of ε_3 taking ε_2 in the set $R_2 = \{\varepsilon_2; \varepsilon_2 = \varepsilon_3, 10^{-1}\varepsilon_3, \ldots, 10^{-6}\}$ and ε_1 in the set $R_1 = \{\varepsilon_1; \varepsilon_1 = \varepsilon_2, 10^{-1}\varepsilon_2, \ldots, 10^{-7}\}$. From them, we observe the first order of uniform convergence of the numerical algorithm.

6 Conclusions

In this article, we have constructed a numerical algorithm to solve 2D reaction–diffusion parabolic singularly perturbed systems with time dependent Dirichlet boundary conditions. The diffusion parameters at each equation can be distinct and have a different order of magnitude; in these circumstances overlapping boundary layers use to appear. The numerical method combines the central finite differences scheme

Figure 8: Components at $t = 1$ for example (21) with $\varepsilon_1 = 10^{-6}$, $\varepsilon_2 = 10^{-4}$, $\varepsilon_3 = 10^{-2}$ and $N = 48, M = 32$ (left u_1, center u_2, right u_3)

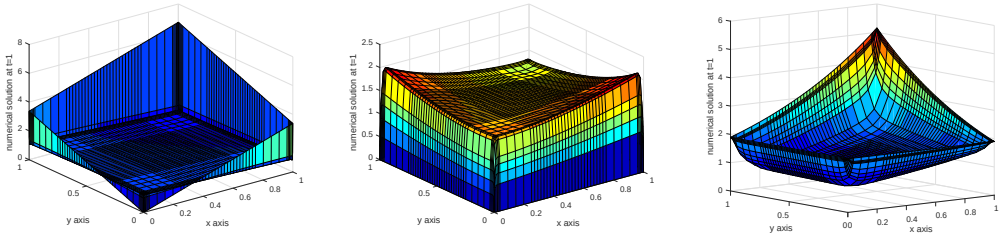

Table 3: Estimated maximum errors using the double mesh principle and orders of convergence for the first component of example (21)

ε_3	N=36 M=8	N=72 M=16	N=144 M=32	N=288 N=64
10^{-1}	4.4486E-1 0.1125	4.1148E-1 0.4515	3.0090E-1 0.9913	1.5136E-1
10^{-2}	4.4552E-1 0.1149	4.1140E-1 0.4514	3.0087E-1 0.9912	1.5135E-1
10^{-3}	4.4309E-1 0.1081	4.1109E-1 0.4507	3.0078E-1 0.9910	1.5133E-1
10^{-4}	4.4308E-1 0.1100	4.1055E-1 0.4497	3.0059E-1 0.9906	1.5127E-1
10^{-5}	4.4308E-1 0.1124	4.0986E-1 0.4491	3.0021E-1 0.9900	1.5115E-1
$d_1^{N,M}$ p_1^{uni}	4.4552E-1 0.1147	4.1148E-1 0.4515	3.0090E-1 0.9913	1.5136E-1

to discretize in space and the fractional implicit Euler method together a splitting by components to discretize in time. If the method is defined on appropriate piecewise uniform Shishkin meshes in space, then the fully discrete scheme is uniformly convergent of first order in time and almost second order in space. The use of a special discretization of the boundary data eludes the order reduction phenomena associated to classical discretizations. Moreover, the time integrator proposed provokes that only linear tridiagonal systems must be solved at each time level, which supposes a remarkable reduction in the computational cost in comparison with classical implicit methods. Numerical tests show the reliability of our proposal, as the theoretical results predict.

Table 4: Estimated maximum errors using the double mesh principle and orders of convergence for the second component of example (21)

ε_3	N=36 M=8	N=72 M=16	N=144 M=32	N=288 N=64
10^{-1}	1.9747E-1 0.8252	1.1145E-1 0.6942	6.8883E-2 0.8148	3.9159E-2
10^{-2}	1.9749E-1 0.8136	1.1237E-1 0.6980	6.9264E-2 0.8189	3.9265E-2
10^{-3}	1.9774E-1 0.7979	1.1374E-1 0.6925	7.0380E-2 0.8338	3.9487E-2
10^{-4}	1.9845E-1 0.9273	1.0435E-1 0.6880	6.4772E-2 0.8281	3.6485E-2
10^{-5}	1.5895E-1 0.7808	9.2521E-2 0.8855	5.0080E-2 0.8008	2.8748E-2
$d_2^{N,M}$ p_2^{uni}	1.9845E-1 0.8030	1.1374E-1 0.6925	7.0380E-2 0.8338	3.9487E-2

Acknowledgements

This research was partially supported by the project MTM2017-83490-P and the Aragón Government and European Social Fund (group E24-17R).

References

[1] C. Clavero, J.L. Gracia, Uniformly convergent additive schemes for 2D singularly perturbed parabolic systems of reaction-diffusion type, Numer. Algorithms **80** (2019) 1097–1120.

[2] C. Clavero, J.C. Jorge, Solving efficiently one dimensional parabolic singularly perturbed reaction-diffusion systems: a splitting by components, J. Comp. Appl. Math **344** (2018) 1–14.

[3] C. Clavero, J.C. Jorge, An efficient numerical method for singularly perturbed time dependent parabolic 2D convection-diffusion systems, J. Comp. Appl. Math. **354** (2019) 431–444.

[4] C. Clavero, J.C. Jorge, Numerical approximation of 2D time dependent singularly perturbed reaction-diffusion systems: an efficient uniformly convergent method, in preparation.

[5] C. Clavero, J.C. Jorge, F. Lisbona, G.I. Shishkin, An alternating direction scheme on a nonuniform mesh for reaction-diffusion parabolic problems, IMA J. Numer. Anal. **20(2)** 263–280 (2000).

Table 5: Estimated maximum errors using the double mesh principle and orders of convergence for the third component of example (21)

ε_3	N=36 M=8	N=72 M=16	N=144 M=32	N=288 N=64
10^{-1}	1.2078E-1 1.0516	5.8268E-2 0.9503	3.0155E-2 0.9020	1.6138E-2
10^{-2}	1.6958E-1 1.0638	8.1122E-2 1.0107	4.0260E-2 0.9819	2.0385E-2
10^{-3}	2.0717E-1 0.8347	1.1616E-1 1.1113	5.3766E-2 1.2734	2.2242E-2
10^{-4}	2.1191E-1 1.1337	9.6580E-2 1.0955	4.5196E-2 1.0528	2.1787E-2
10^{-5}	1.4657E-1 1.0159	7.2485E-2 0.9990	3.6266E-2 1.0055	1.8065E-2
$d_3^{N,M}$ p_3^{uni}	2.1191E-1 0.8674	1.1616E-1 1.1113	5.3766E-2 1.2734	2.2242E-2

[6] P.A. Farrell, A.F. Hegarty, J.J.H. Miller, E. O'Riordan, G.I. Shishkin, Robust Computational Techniques for Boundary Layers, Applied Mathematics, **16**. Chapman and Hall/CRC, (2000).

[7] J.L. Gracia, F. Lisbona, A uniformly convergent scheme for a system of reaction–diffusion equations, J. Comp. Appl. Math. **206** 1–16 (2007).

[8] J.L. Gracia, F. Lisbona, E. O'Riordan, A coupled system of singularly perturbed parabolic reaction-diffusion equations, Adv. Comput. Math. **32** 43–61 (2010).

[9] R.B. Kellogg, T. Linss, M. Stynes, A finite difference method on layer-adapted meshes for an elliptic reaction-diffusion system in two dimensions, Math. Comput. **774** (2008) 2085–2096.

[10] R.B. Kellogg, N. Madden, M. Stynes, A parameter robust numerical method for a system of reaction-diffusion equations in two dimensions, Numer. Meth. Part. Diff. Equa. **24** (2007) 312–334.

[11] N. Madden, M. Stynes, A uniformly convergent numerical method for a coupled system of two singularly perturbed linear reaction-diffusion problems, *IMA J. Numer. Anal.* **23** (2003) 627–644.

[12] O.A. Ladyzhenskaya, V.A. Solonnikov, and N.N. Uraltseva, Linear and Quasilinear Equations of Parabolic Type, Translations of Mathematical Monographs, **23**, American Mathematical Society, Providence, R.I. (1967).

[13] C.V. Pao, Nonlinear parabolic and elliptic equations, Plenum Press, New Yotk (1992).

[14] H.G. Roos, M. Stynes, L. Tobiska, Robust numerical methods for singularly perturbed differential equations, Springer Series in Computational Mathematics, Berlin (2008).

[15] G.I. Shishkin, Approximation of systems of singularly perturbed elliptic reaction-diffusion equations with two parameters, *Comput. Math. Math. Phys.* **47** (2007) 797–828.